Supplementary Material

Thermoelectric enhancement by intramolecular rotation in tetraphenylporphyrin-based molecular junctions

Yongfeng Xiong[1], Zhenhai Cui[2], Min Li[1], Tong Chen[1], Lin Huang[1]*

[1]*School of Energy and Mechanical Engineering, Energy materials computing center, Jiangxi University of Science and Technology, Nanchang 330013, China*

[2]*School of Software Engineering, Jiangxi University of Science and Technology, Nanchang 330013, China*

*Corresponding author (Lin Huang): linhuang@jxstu.edu.cn

1. Convergence tests under different calculation parameters of the tetraphenylporphyrin (TPP) molecular devices at different rotation angles.

Fig. S1 displays determine the transmission spectra of the structures of Sr and Dr under different rotation angles for the four sets of calculation parameters: 3*3 K point, 5*5 K point, cutoff energy of 200 Ry, and SCF convergence of 10^{-6}.As can be seen from the figure, changing the calculation parameters does not significantly affect the size change of the rotation at point EF. Therefore, this transport property has basically stabilized.

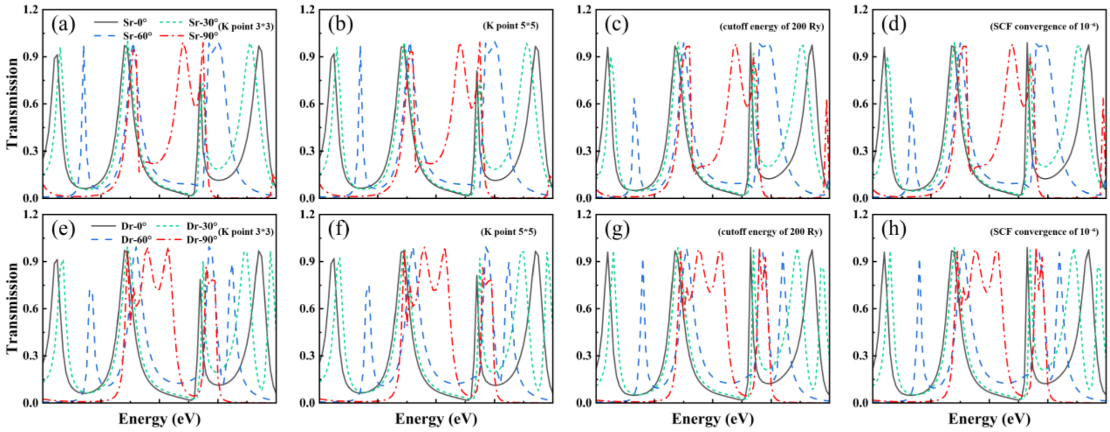

Fig. S1 Electron transmission spectra of MJs under different rotation angles for Sr and Dr configurations.

2. Molecular dynamics calculations of the force field of the tetraphenylporphyrin (TPP) molecular devices at different rotation angles.

Fig. S2 displays the molecular dynamics simulation of the oscillation of NVT Nose Hoover heat bath energy over time of the Sr and Dr configurations at various rotation angles.The results show that increasing the rotation angle leads to higher total energies accompanied by an initial structural relaxation, during which the torsion angle partially decreases toward lower-energy configurations. After this relaxation, the systems reach stable fluctuation plateaus, indicating that large-angle configurations correspond to thermodynamically less favorable but dynamically accessible metastable states under constrained conditions. During dynamical evolution, the junction tends to relax toward the initial low-energy configuration, suggesting that large-angle rotated structures correspond to metastable or mechanically constrained states.

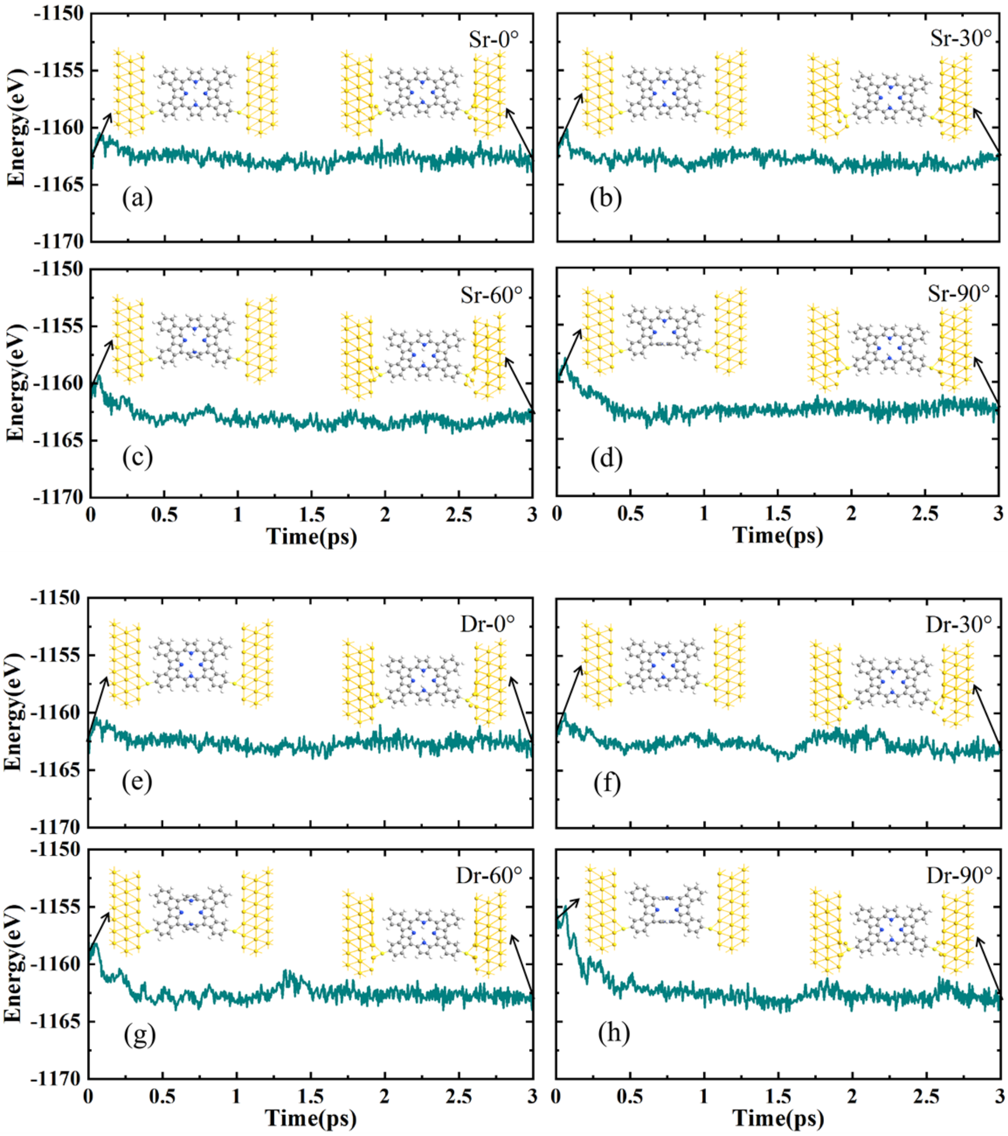

Fig. S2 The oscillation of energy over time of MJs under different rotation angles for Sr and Dr configurations.

3. The transmission pathway of the tetraphenylporphyrin (TPP) molecular devices at different rotation angles.

To examine the magnetism induced by a 90° rotation of the Sr and Dr configurations, we calculated the projected density of states (PDOS) of their device spin states under zero bias, as shown in Fig. S3. As shown in Fig. S3(a)-(c), (e)-(g), the PDOS of the three molecular junctions exhibits complete degeneracy on both the molecules and the bonded sulfur atoms, indicating the absence of magnetism in the system. However, when the rotation angle increases to 90° (in Fig. S3(d)(h)), the frontier states near EF gradually develop weak spin polarization. This suggests that molecular rotation breaks the spin symmetry of the system, thereby inducing spin-selective electron transport in the junctions.

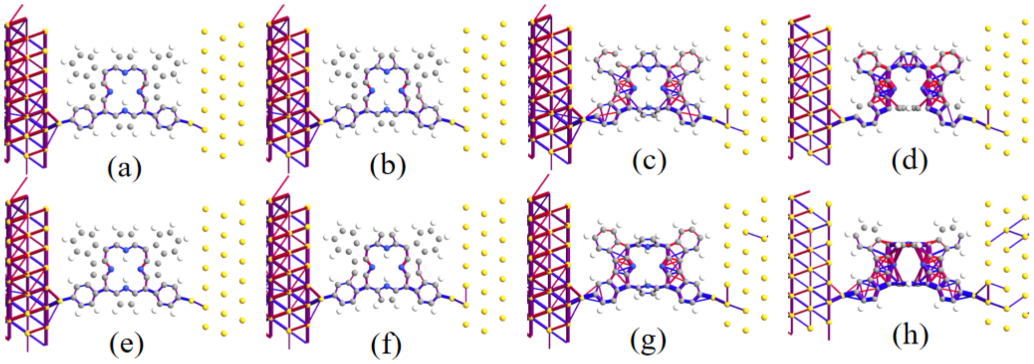

Fig. S3 The transmission pathway of MJs under different rotation angles for Sr and Dr configurations at zero bias. The upper panels correspond to the Sr configurations at different rotation angles, while the lower panels correspond to the Dr configurations.

4. The spin-resolved electron transmission spectra of the tetraphenylporphyrin (TPP) molecular devices at rotate 90°.

As shown in Figure. S4(a), the Sr-90° system exhibits a distinct spin-splitting feature near the Fermi level. The transmission peaks for spin-up and spin-down channels no longer coincide, particularly showing a pronounced shift in the energy regions near the HOMO (left of the Fermi level) and the LUMO (right of the Fermi level). This observation indicates that the system transitions from a nonmagnetic to a magnetic state upon a 90° rotation, where spin polarization causes an asymmetric distribution of the electronic density of states between the two spin channels. The spin-dependent transmission splitting originates from the disruption of π-conjugation and the reconstruction of the molecule–electrode coupling induced by molecular rotation, which localizes part of the electrons and gives rise to a net spin moment.As shown in Figure S4(b), the spin splitting in the Dr-90° system becomes more pronounced, with an even larger energy difference between the spin-up and spin-down transmission peaks. Meanwhile, the overall transmission intensity is lower than that of the Sr system, indicating that the double rotation leads to a more distorted molecular plane, weaker molecule–electrode coupling, and more restricted electron transport channels. Although the overall transmission coefficient decreases, the stronger spin splitting indicates a more pronounced spin-polarization effect, which may result in better spin selectivity in spin-dependent thermoelectric (spin-Seebeck) applications.

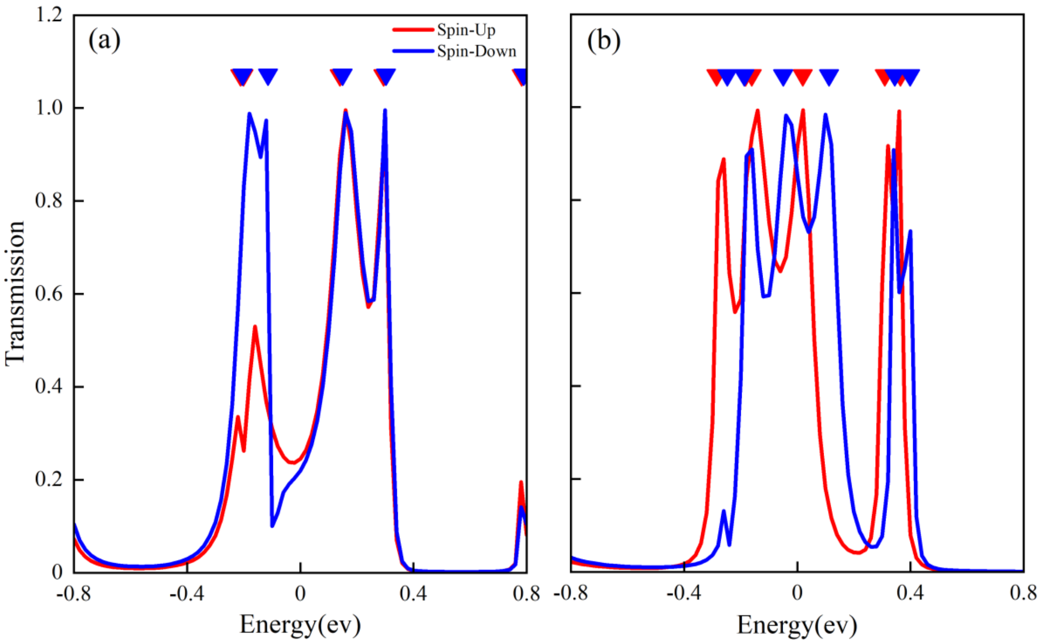

Fig. S4 Spin-resolved electron transmission spectra for Sr and Dr configurations under the rotation angle of 90°.

5. The electronic density distributions of the tetraphenylporphyrin (TPP)

molecular devices at rotate 90°.

As shown in Fig. S5(a), In the Sr configuration. The system transitions from a non-magnetic to a magnetic state. The main reason for this is that as the rotation angle increases, the π-conjugated structure of the central molecule is disrupted, and the electronic coupling between molecular planes is significantly weakened, leading to the breaking of orbital degeneracy and a reduction in the energy gap between the HOMO and LUMO. At this point, some electrons are localized on the local π orbitals, resulting in an asymmetric distribution of spin-up and spin-down electron densities, thereby inducing the formation of a spontaneous magnetic moment. This process is essentially an electronic degeneracy breaking effect caused by molecular structural distortion, transforming the system from a closed-shell to an open-shell state. Additionally, in the Dr configuration, the conjugation disruption caused by this rotation is more pronounced, and the electron cloud shows a stronger localization trend in the central region, thus the magnetization effect is more significant compared to the single-rotation system.

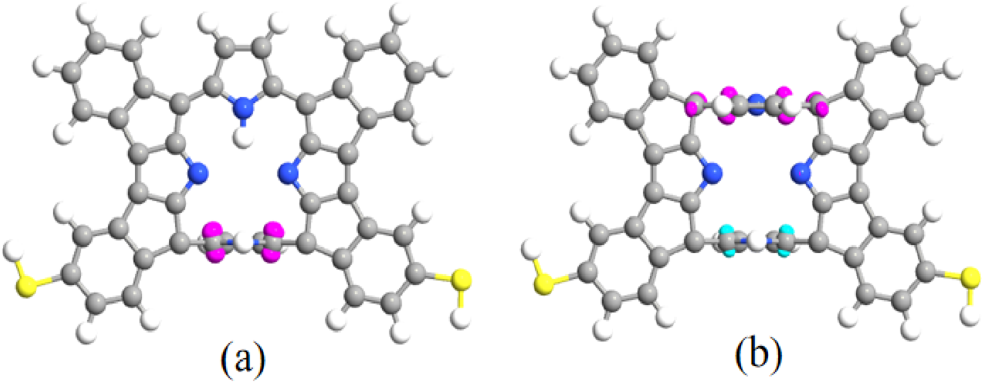

Fig. S5 (a)-(b) Spin electron density distribution for Sr and Dr configurations under the rotation angle of 90°.

6. The spin-resolved projected density of states (PDOS) of the tetraphenylporphyrin (TPP) molecular devices at different rotation angles.

To examine the magnetism induced by a 90° rotation of the Sr and Dr configurations, we calculated the projected density of states (PDOS) of their device spin states under zero bias, as shown in Fig. S6. As shown in Fig. S6(a)-(c), (e)-(g), the PDOS of the three molecular junctions exhibits complete degeneracy on both the molecules and the bonded sulfur atoms, indicating the absence of magnetism in the system. However, when the rotation angle increases to 90° (in Fig. S6(d)(h)), the frontier states near E_F gradually develop weak spin polarization. This suggests that molecular rotation breaks the spin symmetry of the system, thereby inducing spin-selective electron transport in the junctions.

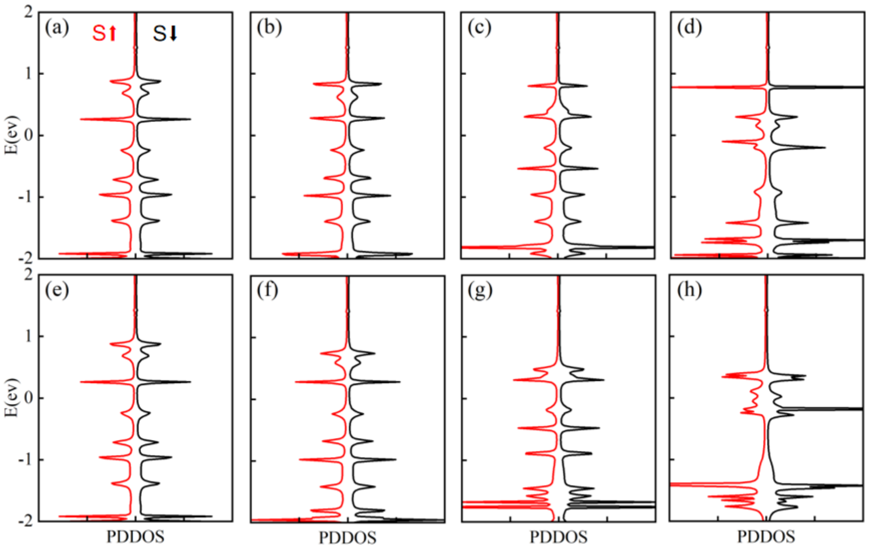

Fig. S6 (a)-(d), (e)-(h) Spin-resolved projected density of states (PDOS) of MJs under different rotation angles for Sr and Dr configurations.

7. Spatial distributions of the frontier MPSH orbitals of the tetraphenylporphyrin (TPP) molecular devices at different rotation angles.

Fig. S7 displays the molecular projected self-consistent Hamiltonian (MPSH) orbitals of the Sr and Dr configurations at various rotation angles. In the Sr configuration, as the molecular rotation angle varies, both the HOMO and LUMO exhibit significant amplitude extension at the molecular-electrode interface, indicating that these frontier orbitals (and their adjacent states) are well-coupled with the electrodes, serving as the primary transport channels under low bias. At the 90° conformation, the HOMO orbital displays a highly localized distribution, thereby suppressing transmission and generating narrow and weak resonance peaks. The

LOMO orbital maintains angular similarity with other angles, demonstrating good electrode coupling, thus the transmission is predominantly governed by the LOMO. In the Dr configuration, different rotation angles exhibit identical properties (except at 90°). At the 90° conformation, the HOMO distribution remains largely unchanged, while the LOMO distribution becomes more delocalized, thereby enhancing transmission.

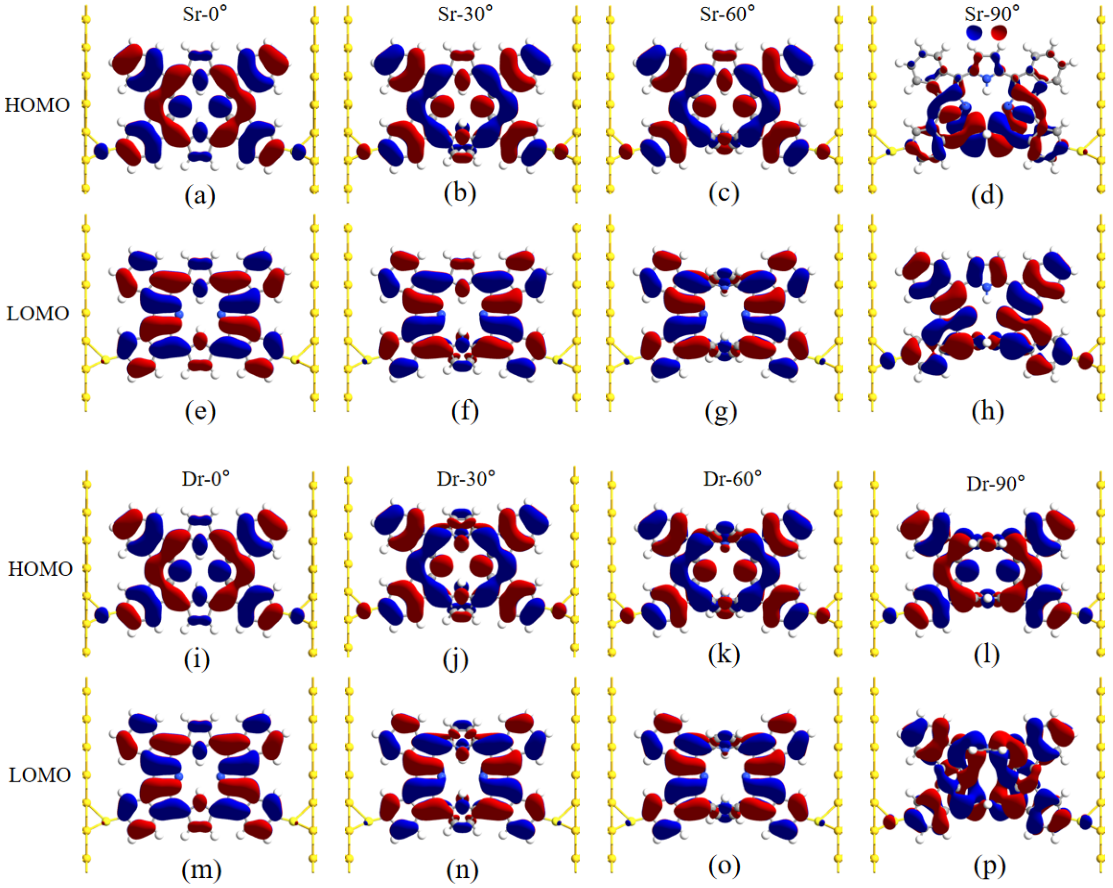

Fig. S7 Spatial distributions of the frontier MPSH orbitals of MJs under different rotation angles for Sr and Dr configurations.The red and blue colors represent the positive and negative phases of the molecular orbitals, respectively. An isovalue of 0.03 a.u. is used.